Rotor to stator contacts in turbomachines. Review and application

Georges Jacquet-Richardet, Mohamed Torkhani, Patrice Cartraud, Fabrice Thouverez, Thouraya Nouri-Baranger, Mathieu Herran, Claude Gibert, Sébastien Baguet, Patricio Almeida, Loïc Peletan

Rotor to stator contacts in turbomachines. Review and application

G. Jacquet-Richardet, M. Torkhani, P. Cartraud, F. Thouverez, T. Nouri Baranger, M. Herran, C. Gibert, S. Baguet, P. Almeida, L. Peletan

Rotor to stator contacts in turbomachines. Review and application

G. Jacquet-Richardet [a,*], M. Torkhani [b], P. Cartraud [c], F. Thouverez [d], T. Nouri Baranger [a,e], M. Herran [f], C. Gibert [d], S. Baguet [a], P. Almeida [d], L. Peletan [a,b]

[a] Université de Lyon, CNRS INSA-Lyon, LaMCoS UMR5259, F-69621 Villeurbanne, France
[b] LaMSID Laboratoire de Mécanique des Structures Industrielles Durables, UMR EDF-CNRS 2832, Clamart, France
[c] LUNAM Université, GeM UMR CNRS 6183, Ecole Centrale de Nantes, F-44321 Nantes, France
[d] Ecole Centrale de Lyon, Laboratoire LTDS, F-69134 Ecully, France
[e] Université de Lyon, Université Lyon 1, F-69622 Villeurbanne, France
[f] Turbomeca, F-64511 Bordes, France

The safety of turbomachines requires controlling the risks caused by contacts occurring between fixed and rotating parts. Undesirable phenomena induced by bladed wheel/casing interactions are caused by the forced excitation of the natural modes of a blade leading to its damage or by potentially dangerous couplings between the modes of the casing and those of the wheel. Rotor–stator contacts may also lead to various types of dangerous behavior, including the well known configurations of dry whirl and dry whip. The paper proposes a large-scale literature review and examines existing numerical models and experimental setups used for highlighting the phenomenology involved in different rotor to stator contacts configurations. It confirms the great complexity of the problems which, by nature, are considerably nonlinear and involve multiphysics and multiscale coupled behaviors.

1. Introduction

Turbomachines are used to transfer energy between a rotating assembly, called rotor, and a fluid. They have different designs according to their functions: turbines (energy from fluid to rotor), compressors (energy from rotor to fluid), jet-aircraft engines (Fig. 1), pumps, turbochargers, etc. Nevertheless most of them have common characteristics and their rotors are made of wheels mounted on a common shaft linked to a stationary housing by bearings. The rotor is necessarily spaced from the housing but in order to prevent leakage and to optimize the efficiency of the machine this space shall be kept as small as possible at specific locations, for example between different stages or at the tip of bladed wheels. As a consequence of those small clearances, contact under rotation may occur and such contact, called rub, may result in different damage severity ranging from cosmetic damage to a full destruction of the equipment. The efficiency and safety of turbomachines require controlling the risks caused by possible contacts.

Rub may result from different undesired phenomena, for example unusual high vibrational level of the rotating assembly, different thermal growth between rotor and stator and blade loss. Blade loss causes an instantaneous huge unbalance and within a few revolutions the response grows and severe rubs occur at blade tip and/or at seal locations on the rotor. Rub, once engaged results in a modification in the global systems dynamics that becomes highly nonlinear. In this framework, two main types of configurations, illustrated in Fig. 2, will be considered here.

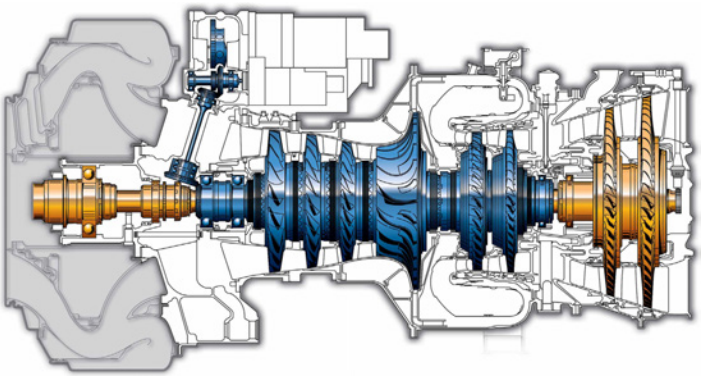

Fig. 1. Helicopter turboshaft RTM322 (Turbomeca–Rolls Royce)—An example of turbomachine.

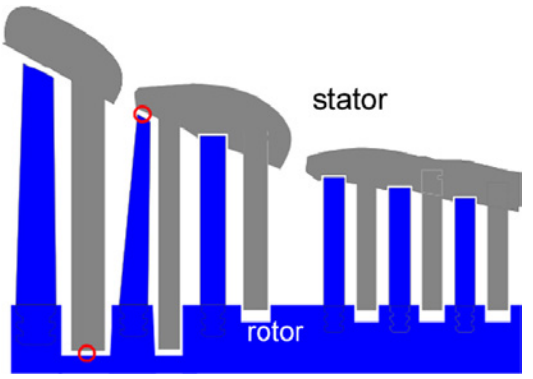

Fig. 2. Possible contacts between rotor and stator/blades and casing.

In the first configuration the contacts between the tip of the blades and the casing, associated with relatively weak force levels, generate an exchange of energy This can lead to different states according to the rotor's speed of rotation, the load and the system's geometrical and physical parameters. These states may induce unstable phenomena whose consequences can be disastrous. The second configuration, associated with high unbalance levels, is generally consecutive to an accidental blade loss. It leads to severe contact between the rotor and the stator that continues while the machine is slowing down. Although rare, this situation must be studied and qualified. Whatever the configuration, in the design phase, it is vital to control the physical phenomena generated during contact and their consequences (breaking, trapped debris, etc.).

A number of studies have been dedicated to the non-linear dynamics of assemblies generated by rotor/stator and blade/casing contacts. However, the associated phenomena are still not fully understood. The main reason is linked to the complex mechanisms involved which are both multi-physical (vibrations, rubbing contact, heating, wear, etc.), multiscale (local/global coupling of dynamic and thermomechanic responses, high rotation speeds), nonlinear (contacts, large displacements, large deformations, significant efforts in bearing structures, plasticity, etc.). The behavior in presence of contacts is therefore characterized by significant interactions between the global dynamics of the system and local phenomena involving material and tribological characteristics (temperature, abradability, etc.).

The objective here is to present the fullest bibliographic synthesis possible regarding the behaviors of rotating machines in presence of rotor/stator and blade/casing contacts. In particular, the aim is to identify the physical phenomena involved, the models adapted and the experimental results available.

2. Physical phenomena—modeling

2.1. Blade-casing contact

In axial and centrifugal compressors, minimizing the clearance between blade tips and the casing that surrounds them increases aerodynamic efficiency but also the risk of potentially destructive contacts. Analysis of the dynamic behavior resulting from blade-casing contacts has been given little attention in the literature. To our knowledge, the first significant study on the subject was published by Schmiechen [1], who carried out modeling and experimental works on simple, axially symmetric structures. This was followed by Sinha [2], who developed an analytical model for calculating the dynamic transient nonlinear behavior associated with critical speeds during acceleration and deceleration. This model was then used for stability analyses [3,4]. Approaches based on finite element models have also been developed, first in [5], to predict with greater precision the range of vibratory behaviors associated with contacts.

Undesirable phenomena induced by bladed wheel/casing interactions are caused by the forced excitation of the natural modes of a blade leading to its damage or by potentially dangerous couplings between the modes of the casing and those of the wheel [6]. The different states associated with rubbing conditions can be classified as damped (the contacts disappear through time), divergent (the amplitude of the vibrations increases constantly) and self-maintained (the contacts do not disappear through time). In the latter case, two types of behavior have been highlighted according to whether the contacts are permanent, intermittent or blocked [6].

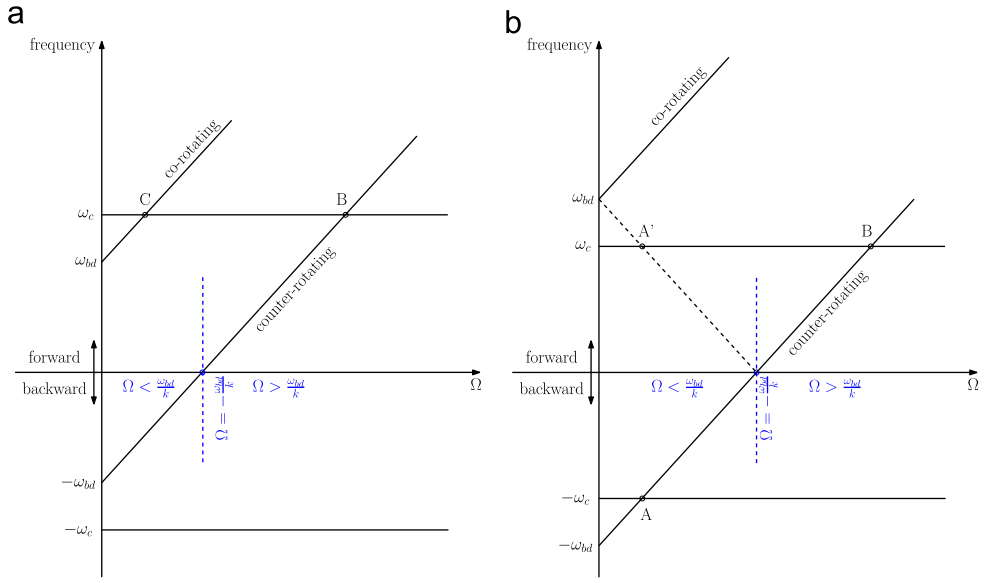

Fig. 3. Interaction diagrams in fixed frame. Possible interactions A, B and C.

In the case of an intermittent contact, a blade touches the casing after which the contact disappears and is followed by a new contact, by the same or another blade. This situation involves modal interaction in which blades and casing undergo deformations that can couple with an exchange of energy that can lead to highly destructive configurations. For this type of interaction to occur, a coincidence of traveling wave speeds is required [1]. The rotor's speed of rotation (Ω_c) must be linked to the vibration of the interacting bodies as a function of the general relation $\Omega_c = |\omega_c + / - \omega_{bd}|/k$, where ω_c is the natural frequency of the mode of the casing and ω_{bd} the natural frequency of the mode of the bladed wheel [5,6]. Parameter k represents the number of nodal diameters, since energy can only be exchanged in the case of two modes with the same number of diameters. According to Schmiechen [1] co and counter rotating waves are related to the rotating frame while forward and backward waves are related to the stationary frame and associated respectively with positive and negative frequencies.

The general relation given above implies three possible interaction cases and may be illustrated by interaction diagrams such as those presented in Fig. 3. Case A where $\Omega_c = (\omega_{bd} - \omega_c)/k$ is generally not considered since it happens far from operating ranges. At low rotational speed, the initialization of interactions should not occur as centrifugal and dynamic effects are too weak to generate contact. Legrand [6] does not take into account this possibility as frequencies of axial compressor casings are generally higher than those of the associated bladed wheels. Case B where $\Omega_c = (\omega_{bd} + \omega_c)/k$ is associated to the coincidence between a forward casing mode and a counter rotating wheel mode. During modal interaction at high rotational speed, the action–reaction principle implies that the friction forces between the two structures are oriented in the direction of rotation on the casing and in the opposite direction on the blades. Such condition is required for the rotational energy of the rotor to be transferred to the vibrating system [6].

As presented in Fig. 4 the bladed assembly is rotating anti-clockwise at speed Ω_c (rotational direction illustrated by the motion of the black blade). In this case the contact induces an interaction between a forward mode with three diameters at speed ω_c/k on the casing (the black dot shows the position of one of the nodal diameters) and a counter rotating mode at speed $\Omega_c - \omega_{bd}/k$ on the wheel (note that such a wave is forward in the fixed frame). Finally case C where $\Omega_c = (\omega_c - \omega_{bd})/k$ is, as case A, generally not considered since it happens also within speed ranges where contact cannot be initialized.

Modal interaction has been identified as the probable cause of the accident that occurred on 3 November 1973 on National Airlines flight 27 from Miami to San Francisco. The DC-10 was flying at cruising speed at 39,000 feet when engine number 3 completely disintegrated (http://accidents-ll.faa.gov/ll_main.cfm?TabID=3&LLID=19&LLTypeID=2).

Another important case to be considered is that of a configuration in which the casing is mechanically insensitive to interaction. It therefore behaves like a deformed but rigid structure. Thus the modal interaction occurs when the speed of

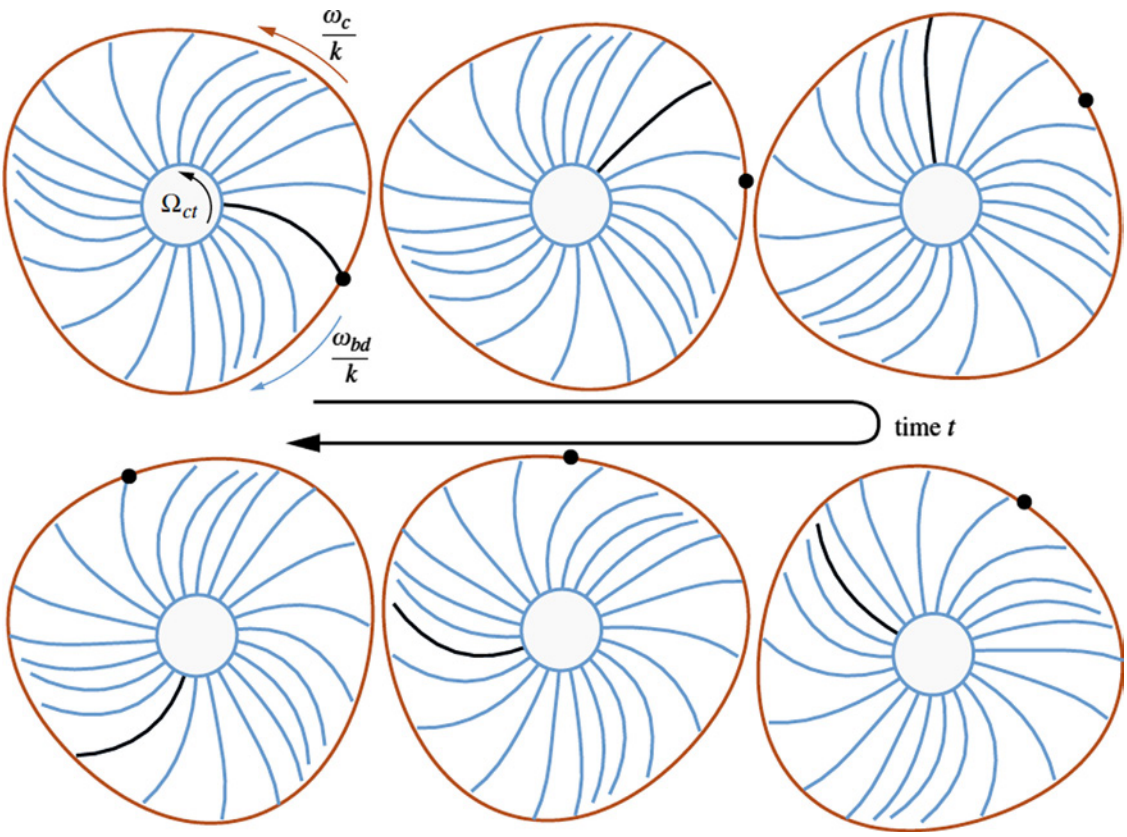

Fig. 4. Illustration of the phenomenon of modal interaction for a case with three diameters [6].

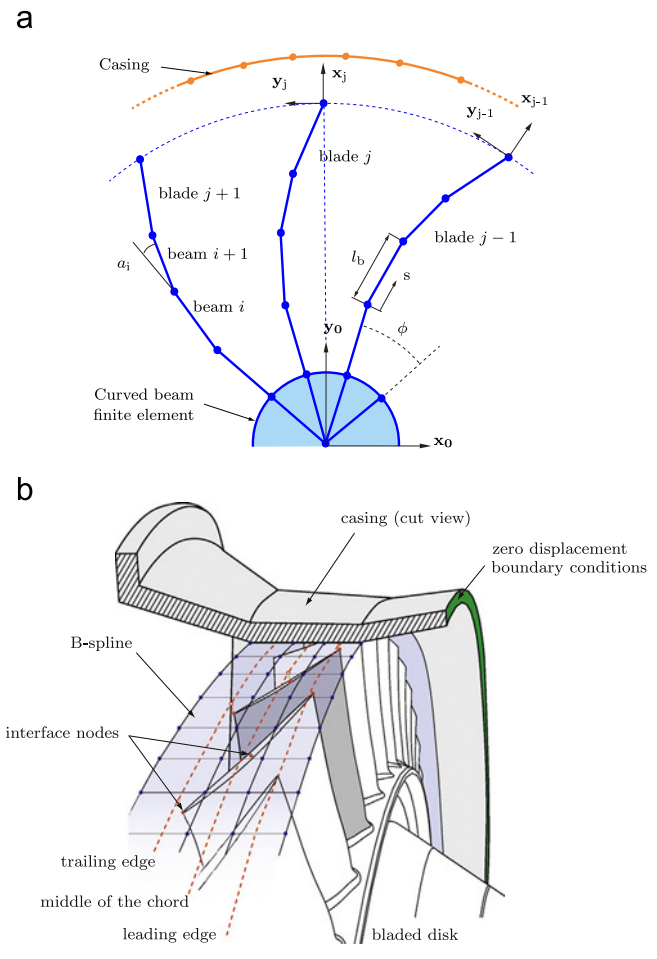

Fig. 5. Plane beam and three dimensional models [10,12].

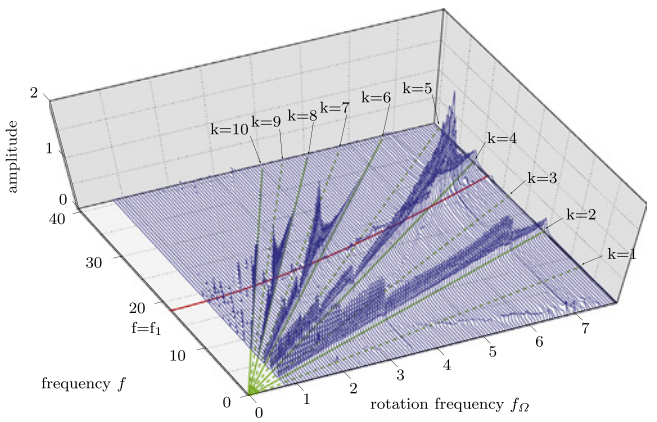

Fig. 6. Spectrum of the radial displacement at blade tip of a node at the leading edge for a casing deformed according to a profile with 2 diameters [11].

the rotor is synchronized with the blade's vibrational frequency, I.e. $\omega_{bd}=k\Omega_c$, which corresponds to the specific case of the previous relation when $\omega_c=0$. This leads to the formation of wear patterns, as shown in [7], patterns whose contact excites in this case both the modes of first bending and first torsion, consuming clearance at the leading edges and trailing edges of the blades respectively. These results are also reproduced by numerical simulation in Ref. [8]. This situation is usually encountered at engine low rate and the design of blades must be capable to sustain it. In Ref. [9] the amplitude of the response of two compressor blades are compared and the robustness of a redesigned blade is confirmed.

The phenomenon of interaction between rotating blade tips and the casing is considerably nonlinear and difficult to model analytically. Several simplified numerical approaches, based on beam type models for the casing and the blades, have been proposed and are illustrated in Fig. 5 [4,6,10]. These models are able to reproduce the interaction phenomena mentioned previously, but in general they do not take into account unbalance and gyroscopic effects. More realistic models incorporate the contact phenomenology and its three dimensional kinetics [6], with the contact surface described at the level of the casing by B-splines. Considering their complexity, these models are associated with modal reduction techniques (CMS Component Mode Synthesis) in order to reduce the size of the problem to be solved. Different types of method may be used, for example as in Refs. [10,11] a fixed interface Craig–Bampton method and a free interface Craig–Martinez method. These two methods give good approximations of the motion at blade tips. The Craig–Bampton method, however, is the most efficient for industrial applications. By using this type of approach, it is possible to obtain the response spectrum of a rotor–stator assembly within a range of rotation speeds (Fig. 6) at reduced cost.

The local contact law plays a decisive role for these interaction phenomena. Contact occurs through a specific coating. Current turbomachines are equipped with abradable type coatings that limit the stresses applied to the blades while optimizing the clearance between the blades and the casing. Zheng [13], Batailly [14], Williams [9] and Millecamps [15,16] focused on modeling abradable coatings. The first used a plasticity law to control wear, whereas the second considered a linear erosion law and the latter relied on finite element simulations that incorporate an Archard type law, blade dynamics, heating and thermal expansion. These studies allow testing abradable coatings in relation to the dynamics induced in the blades in contact. Batailly and Legrand [8] proposed an approach based on an elastoplastic model of the coating, taking into account the variability of blade-casing clearance. Williams [14] showed that the increase in abradable coating density increases the amplitudes of vibrations but also that the geometrical design of the blades has a considerable influence on contact forces and thus on the mechanical behavior of the assembly.

2.2. Rotor–stator contact

2.2.1. Observed behaviors

Muszynska [17,18] and Ahmad [19] provide a literature review on the characterization of rotors with severe unbalance in rubbing type situations. The range of scenarios considered covers occasional contacts with friction to annular rubbing, including the violent phenomenon associated to backward whirl. Feedback from experience has highlighted three main types of behavior.

Forward whirl annular motion. In this case the rotor is maintained in contact with the stator and sliding occurs during the full precession. The full annular friction generally occurs in forward whirl at the same speed as that of rotor rotation (forward synchronous whirl). This motion results from the nonlinear response of the rotor due to unbalance, combining centrifugal forces, elastic forces, contact and friction forces.

Backward whirl motion. This configuration in which the rotor is driven in backward whirl in the stator is initiated by friction induced at the contact interface [20]. The rotor rolls or slides continuously on the contact surface and is subject to backward whirl at nonsynchronous speed. Backward whirl is therefore characterized by a frequency that is neither linked harmonically to the frequency of shaft motion, nor to the excitation frequency. The configuration of rolling without sliding is known as dry whirl while the unstable configuration induced by friction is called dry whip. The vibration of the rotor is considerably impacted by friction at the interface. During operation, vibratory levels may stabilize around a constant average value or tend to increase continuously, leading to instability. During contact, the friction forces applied at the zone of interaction drive the rotor in the direction of backward whirl. If, for example, at the moment of contact, the rotor rotates in this direction or if friction is sufficiently high to drive the rotor in this direction, friction forces take the same direction as the movement. In this case a transfer occurs between the rotational energy and the lateral vibration of the rotor and therefore tends to continuously amplify the vibration. This situation lasts until the speed of whirl becomes higher than that of the circumferential speed of the rotor in contact. Then the relative speed changes in sign which reverses the direction of the friction forces in opposition to the precession of the rotor, dissipating energy. The amplitude of vibration therefore tends to decrease until the relative speed changes the sign at the contact again, which will again tend to increase the amplitude of vibration. In this context, the amplitude of the rotor oscillates around a value corresponding to zero relative speed at the contact and vibration becomes self-excited. Once started, this phenomenon is maintained and, when slowing down, it only disappears at very low speed when the relative sliding speed remains constantly close to zero.

The frequency corresponding to dry whip is very close to that of the coupled rotor/stator system. This observation requires very good estimation of the stator's stiffness in the models.

Unbalance has no effect on the phenomenon once engaged but it does affect the conditions of engagement (speed of rotation). Bently [21] demonstrated experimentally that for the same rotor, the rigidity of the mounting can play a considerable role. Annular rubbing in backward whirl can be easily obtained with a very rigid mounting but not with a flexible one.

Rebounds Partial friction is characterized by discontinuous contact along the precession of the rotor and then repeated rebounds between the rotor and the stator. The rebound configuration can be either permanent or transient. The onset of annular rubbing behavior as well as changes in precession always occurs via a transient phase. The amplitudes of the rebound increase as unbalance increases. Thus when unbalance is excessive rebounds cannot be contained within the space

left by the clearance and the transition to annular rubbing is inevitable. Rebound state can be chaotic, quasiperiodic and even periodic. The latter two configurations are those most treated. They imply the presence of subharmonic or superharmonic components of rotational speed. A distinction can be made between the case of responses with periodic impacts generating sub- and super-harmonic components of the synchronous frequency and asynchronous periodic impacts. For the second type, Cole [22] showed that if the movement of the rotor does not exhibit periodicity in the fixed frame, it may become periodic once transformed into the rotating frame.

The existence of different phases of behavior and their limits of appearance and disappearance depend on the parameters of the system. Possible responses vary from periodic to chaotic configurations [23]. Analysis of the motion signals reveals multiple harmonics 2X, 3X…, semi-harmonics such as X/2, 3X/2…. and even third harmonics of type X/3, 2X/3.

Lingener [24] studied an unbalanced rotor during speed increase and decrease. He first observed motion without rubbing, then a zone of synchronous annular rubbing and finally a return to friction-free conditions. The phenomenon of frequency jump was observed when rubbing. During the experiment, he noted that the contribution of an external excitation (shock on the rotor) can change the synchronous response at any moment to annular rubbing type behavior in backward whirl. Once engaged, the movement occurs in rolling configuration without sliding at a supersynchronous frequency equal to the synchronous frequency multiplied by a coefficient equal to the ratio of the rotor radius over the clearance. Under acceleration, the supersynchronous line is followed until reaching a threshold at which friction occurs. Beyond this threshold, the amplitudes increase and the frequency remains constant (dry whip). The threshold is linked to the combined frequency of the rotor–stator system.

Crandall [25] observed that the dry whip phenomenon can set in without external disturbance but may be induced by unbalance and the history of the motion. When unbalance is substantial the contact forces generated are self-sufficient for initiating and maintaining the phenomenon. When unbalance is weaker, initiation requires external disturbance.

Wilkes [26] showed experimentally that the constant frequency associated with dry whip can, during acceleration, end with a jump leading to a return to a whirl type behavior. Continuing acceleration can highlight several alternations between whip and whirl with a jump at each transition [27]. These transitions were not detected in the previous studies performed by the same team on the same system [28]. Here too, the explanation is linked to the influence of initial conditions. The first study dealt with a contact occurring through the continuous increase of vibration amplitudes whereas the latter was based on a pulsed radial disturbance.

Cole [29] showed that with the same starting configuration, very different responses can be obtained as a function of initial conditions.

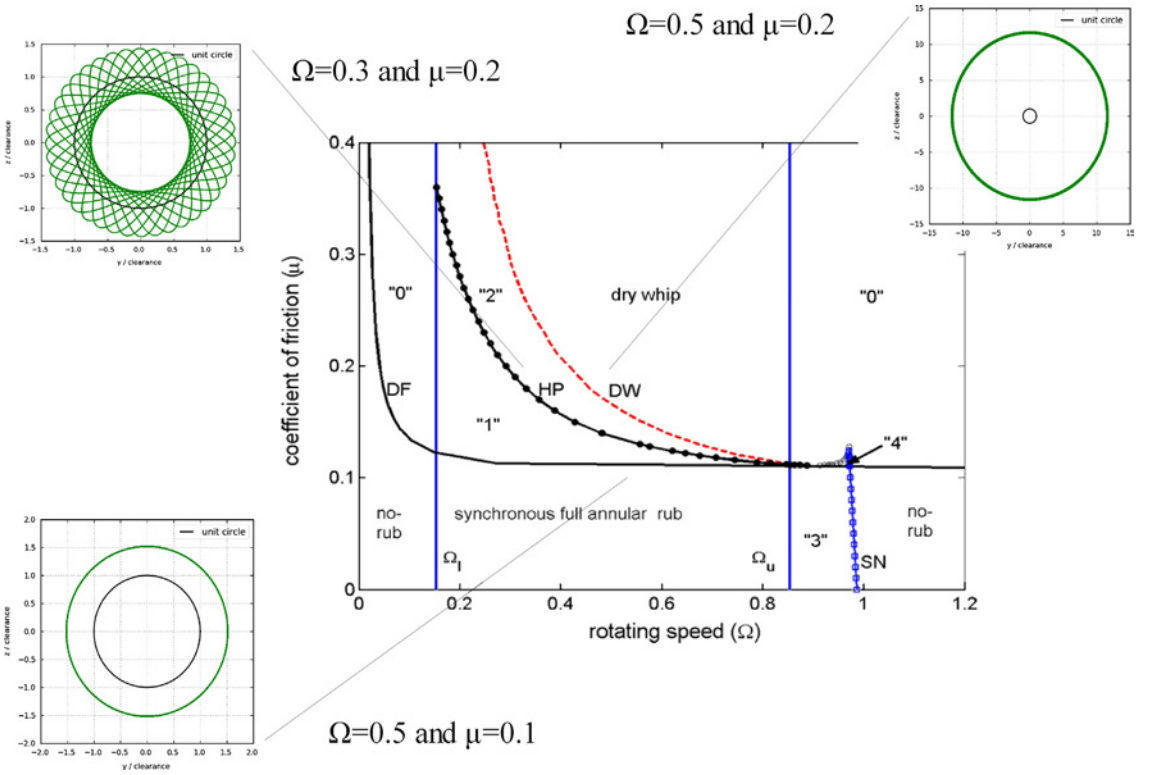

Fig. 7. Characteristics of response as a function of parameters Ω and μ from [32].

Li [30] demonstrated that contact and friction configurations are complex and greatly influenced by the friction coefficient and the eccentricity caused by unbalance. For certain associations of these parameters, the rotor comes into contact with the casing in direct whirl or backward whirl, whereas other values generate annular friction.

Jiang and Shang [31–33] justified the occurrence of different scenarios by highlighting operating zones in which different possible behaviors co-exist (Fig. 7). They explained the jump phenomenon by the existence of zones in which behavior without friction and synchronous annular rubbing co-exist (zone "3" in Fig. 7). They showed that for certain zones dry whip is the only stable configuration. Fig. 7 also shows several orbits corresponding to characteristic configurations. For $\Omega=0.5$ and $\mu=0.1$ the rotor is in synchronous annular whirl. The clearance, indicated by the black circle equal to unity, is slightly exceeded. When $\Omega=0.3$ and $\mu=0.2$ rebound and annular friction in backward whirl configuration may both occur. In this case the rotor penetrates the stator with a significant depth. Lastly, for $\Omega=0.5$ and $\mu=0.2$ the rotor is necessarily in backward annular whirl and the orbits become considerable, clearly illustrating the violence of the phenomenon.

2.2.2. Major parameters involved

Choi focused on the friction coefficient [34]. In this study the coefficient is not fixed a priori but deduced from the system of forces calculated at the contact. The results show a very considerable variation of the friction coefficient as a function of the operating range. Pennachi [35] also observed experimentally a substantial variation of the friction coefficient close to critical speed. Choi [36] specified that the ratio between tangential and normal forces at the contact should not be associated with the friction coefficient. When applying Coulomb's theory, the friction coefficient cannot exceed the classical value associated with the surfaces in presence. A dynamic friction coefficient can be measured by the ratio between tangential and normal forces.

The presence of anisotropies linked, for example, to bearing characteristics, misalignment or external loads, can have a major influence on the behavior of the frictional system [34,36]. To achieve greater realism Popprath [37] considered an offset between the geometrical centers of the rotor and the non-deformed stator without focusing in particular on its effect.

The rigidity of the system plays a major role in the limits of occurrence of backward whirl. Increasing stator rigidity increases friction forces at the interface [38].

Experimental and numerical results converge in establishing that the best way of avoiding the destructive phenomenon of dry whip is to incorporate modal damping as much as possible in the system , to have the lowest possible friction coefficient at the interface and also the lowest possible coefficient of restitution at impact.

2.2.3. Torsional effects and rotational speed variation

Most numerical studies only retain the lateral degrees of freedom expressing the behavior of the rotor in bending.

Al-Bedoor [39] highlighted that considering torsional terms has a significant effect on responses and illustrated the possibility of occurrence of resonance linked to parametric excitations. In particular, he showed that taking into account torsion can lead to increasing the number of resonance peaks in bending. However, related studies are generally based on a very simplified model of a Jeffcott type rotor. Coupled bending/torsion behaviors have been taken into account in studies focusing on cracked rotors. Patel [40] studied this configuration using a beam model and showed the possibility of torsional resonance caused by friction. The study focused on the issue of fault identification (cracks, contact). In addition to the normal and tangential forces at the contact, these models apply a moment of torsion whose expression is obtained by the product of the rotor radius and the tangential force.

Very few works have dealt with the deceleration caused by friction. Pennachi [35] mentions this possibility but does not consider it using the justification that the motor used on the test bench was capable of maintaining constant speed under the study conditions. Grapis [41] proposed a model in which the global changes of kinetic energy are considered and applied in the case of flywheels. During interaction, the kinetic energy is partially dissipated and can also be partially transferred to the kinetic energy of the rotor in bending. Roques [42,43] focused on the case of a steam turbine slowing down after an accidental situation. The finite element model developed takes into account the variable nature of the speed of rotation. A resolution method using time integration was used to calculate the transient response of the shaft line. Rotor–stator contacts occur when passing the critical speed and cause the turbine to decelerate. Braut [44] also focused on deceleration in an accidental situation and presented a coupled numerical–experimental approach.

3. Thermomechanical effects

Thermomechanical models consider the energy dissipated during contact, generally assumed to transform totally into heat [45,46]. The process assumes that there is a distribution of fluxes between the two bodies in contact. Variations of temperature can induce thermal expansions leading to a coupled thermomechanical problem since the geometry is a function of the temperature field, itself influenced by the forces in the contact. As the time constant of the thermal problem is much greater than that of the mechanical problem, it is generally possible to build weakly coupled models, passing from a mechanical resolution to a thermal or thermomechanical resolution.

In the case of shaft–stator contacts, the entire heat flow is applied to the rotor, which seems justified with high relative speeds. The effect is generally localized in the section of the shaft in contact and always at the same point in this section, causing the shaft to bow: thermal bow or Newkirk effect [47]. This phenomenon is the cause of thermal unbalance which, combined with mechanical unbalance, modifies the rotor response. The lateral vibrations are then amplified below the first

critical speed [18]. This gives rise to synchronous spiral movements that can be described mathematically by Kellenberger's model [48] which links the rotor displacements to the temperature at the contact.

The capacity of structures to dissipate heat is also important to reduce the increase of temperature at surfaces and thus their degradation. It appears that the dissipation of heat depends little on the contact force or its speed. However, conductivity and its evolution with temperature, the depth of penetration, the elevation of temperature, and diffusivity are influential parameters.

Abdel-Aal [49] focused on the dissipation of thermal energy due to friction and distinguished a 'flash' temperature at the interface of the structures in contact from a 'bulk' temperature which is sufficiently distant from the surfaces. A heat dissipation model was proposed at the scale of the asperities to obtain a bell shaped distribution of temperature. In Ref. [50] the bulk temperature is considered as the average temperature at the contact surface, whereas the flash temperature is considered as the local temperature of asperities.

For blade/casing contacts with high sliding speeds, the heat flows are mostly applied to the stator. Millecamps [15,16] took into account thermomechanical effects to adjust clearance modified by expansion, and studied their impacts on the dynamic behavior of the assembly. He also considered the influence of wear of the abradable coating. The study is based on a controlled contact configuration in which a blade is longer than the others. The numerical strategy proposed is broken down to several steps. A transient mechanical calculation is first performed during two rotor revolutions. The model includes the overlength blade, the casing and the contact model. From this calculation are extracted the contact forces used to determine, on the one hand the wear of the abradable coating and, on the other, the heat flow generated by the contact. The latter is used in a transient thermomechanical calculation uncoupled from the previous mechanical one. The wear and thermal expansions are evaluated and the system's geometry is updated, making it possible to continue to a new iteration. Initially the abradable coating has a constant thickness and its wear is calculated afterwards, by simply multiplying the normal effort at the contact by a coefficient. The thermomechanical calculations are performed after having determined the flows to be applied to each of the elements by determining their distributions. A constant flow is applied for 1 s, a duration which according to tests corresponds to the duration of thermal phenomena. The results show a partial correlation between the model and the experiment.

Temizer [51] discussed the methodology for characterizing thermal conductivity due to contact at microscopic scale by using the macroscopic variables of the contact.

The possibility of fire caused by the interaction between the blades made of titanium and the casing was dealt with in Ref. [52]. To avoid this phenomenon, a ceramic abradable coating is applied on the blade tips [53].

4. Numerical processing

Several analytical formulations have been developed and used within the frame of rotor/stator interaction. Zhang [54] proposed a formulation adapted to the synchronous annular friction configuration. Jiang [32] developed a more general analytical formulation including different phases of behavior. Grapis [41] dealt with the problem of a flywheel with a rigid rotor and was able to develop a simple analytical model. Childs [28] dealt with steady whirl and whip motions using a reduced model obtained after projection of the rotor equations in modal basis. Such formulations are very useful for specific configurations and for parametric studies. However more general procedures shall be able to deal with finite element models that may be either separated or linked by contact forces. In this case the main choices that have to be done are related to the way contact is considered and the type of numerical scheme used to solve the problem.

4.1. Contact treatment

The simplest model is based on the use of a restitution coefficient that links the speeds of the rotor before and after the contact [55]. This model assumes that the contact is intermittent and that a significant lapse of time separates two successive contacts. More often, contact analyses are performed using different numerical schemes described for example in Ref. [56]:

The Lagrange multiplier method, adds contact constraints between nodes to prevent penetration. With this method, contact conditions are strictly verified apart from possible numerical error. However it leads to increasing the size of the problem as a function of the number of multipliers which remains variable during the process.

With the penalty methods a penetration is accepted and controlled via a penalty coefficient. The external penalty, which permits slight penetration between the structures, is widely used in commercial codes. Using the internal penalty (barrier method) a force prevents the bodies from entering into contact. The penalty methods consider the contact constraints without any increase in the number of degrees of freedom. However the choice of the penalty coefficient plays a major role. A too small value induces imprecision but matrices become ill-conditioned when the value is chosen too high. Studies performed often use an insufficient contact stiffness, in order to improve convergence of numerical schemes. Zhang [54] proposed a technique that ensures a good estimation of this stiffness.

Hybrid or mixed methods combine those basic techniques and alleviate some of their drawbacks. The method using perturbed Lagrangian functions was developed by modifying the contact constraints by external penalty terms. Augmented Lagrangian functions combine the advantages of classical Lagrangian functions and penalty methods. In this case, the condition of non-penetration is respected and the nonlinear problem is equivalent to a constraint free optimization problem.

The Lagrangian multipliers method is used in Refs. [5,6,9,10,42,43]. However, most of the models are based on the penalty method and therefore introduce a contact stiffness between the rotor and the stator when the radial displacement

of the rotor (d) becomes equal to the clearance (e). The contact thus brings an added stiffness k in the radial direction that leads to a restoring radial force $F_n = k(d-e)$. The tangential force associated is generally obtained by using Coulomb's law with friction coefficient μ leading to $F_t = \pm \mu F_n$. The + or – sign used depends on the sign of $\Omega R + V_t$, with Ω being the angular speed of the rotor, R its radius and V_t the speed of the center of the rotor in the tangential direction at contact, counted as positive in the counterclockwise direction. If the sign is positive, the friction force acts in clockwise direction. Models that do not take into account the possible evolution of these signs cannot consider the dry whip phenomenon.

Taking into account a spring–damper system at contact does not raise any problem in principle but in all cases this type of model requires good estimation of the contact stiffness and the damping coefficient. Wikes [26] adjusted the damping coefficient on the basis of experimental results. Popprath [37] established a relation between the stiffness of the spring and the damping coefficient through the shock theory [57]. Thus he could set the stiffness and use it to deduce the damping coefficient. Models including a damper must consider the true separation conditions. Separation corresponds to the moment when the contact force vanishes. Since damping is taken into account, there is no longer any coincidence between the end of penetration and a contact force equal to zero, as the force generally becomes equal to zero just before the end of penetration.

Other models exist for the rotor–stator/blade-casing contact. The Hertz theory assumes that the force at the contact is proportional to $(d-e)\backslash widehat(3/2)$. Such model raises two problems. Its nonlinear character makes it complex to handle and the geometries in contact do not usually conform to the conditions imposed by the theory which assumes that the radii of curvature of the surfaces are not too close. Following on from Popprath [37], Rivin [58] proposed two relations to describe the contact force between two cylindrical surfaces with similar radii. A linear $k(d-e)$ for low force values and $k(d-e)^2$ elsewhere. Wikes [26] modeled the contact force in the form $k_1(d-e)+k_2(de)^2+c(d-e)(d-e)$ derived from the contact theory developed by Hunt and Crossley. Chu [59] focused on the global stiffness of a system at the moment of impact. He identified this stiffness on the basis of numerical and experimental results.

The inclusion of plastic deformations caused by contact is mentioned in several publications that suspect they play a significant role though they have never been implemented.

4.2. Numerical schemes

For numerical analyses involving contacts a distinction can be made between time integration and frequency domain methods. Frequency methods give periodic and quasiperiodic regimes, whereas time integration methods are also capable of determining chaotic regimes.

The Harmonic Balance Method (HBM) is often used when seeking periodic solutions. The efficiency of the method is directly linked to the number of terms considered and the HBM is generally used when a certain amount of information is available beforehand on the behavior of the system. This information is obtained from experience, experiments or preliminary time integration simulations. Experiments often show that the frequency content of responses in operation is

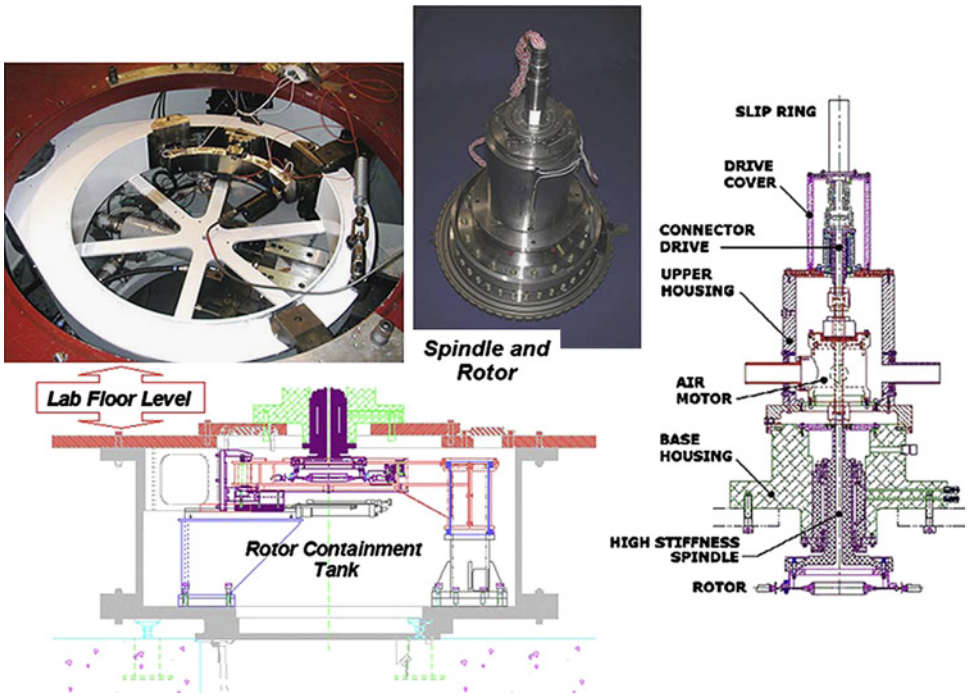

Fig. 8. OSU test bench [70].

limited, justifying the interest in this type of method. Several variants have been developed: HBM applied in the rotating frame using the fundamental contact frequency [22], HBM applied in the fixed frame with arc-length continuation [60], simple HBM [61], HBM with alternating time frequency algorithm [62] (the study neglects friction).

Time methods are based on classical numerical integration procedures: Runge-Kutta [26,34,41,61,63–65], the prediction correction method [39], Newmark [5,6,9,10,35,38,40,42,43,66], time forward integration [37], the Hilbert–Hughes–Taylor implicit method [67]. The use of numerical procedures requires precise detection of the instants of contact and separation. These parameters considerably influence the precision of the results.

To avoid the singularity obtained when relative speed becomes zero, Chen [67] provided a continuous expression for cases in which the relative speed falls below a small value. Cole [29] formulated the motion equations using finite element models in the form of state equations. He analyzed the stability of different solutions associated with critical cases.

5. Experimental results on test benches

Given the complexity of the phenomena and the large number of parameters involved, it is necessary to perform experimental tests to get a better understanding in the physics and to obtain a basis for the validation of numerical models. Test benches are different according to the type of contact under study as reported in Section 2 and the same partition considering first blade-casing contact and then rotor–stator contact will be considered.

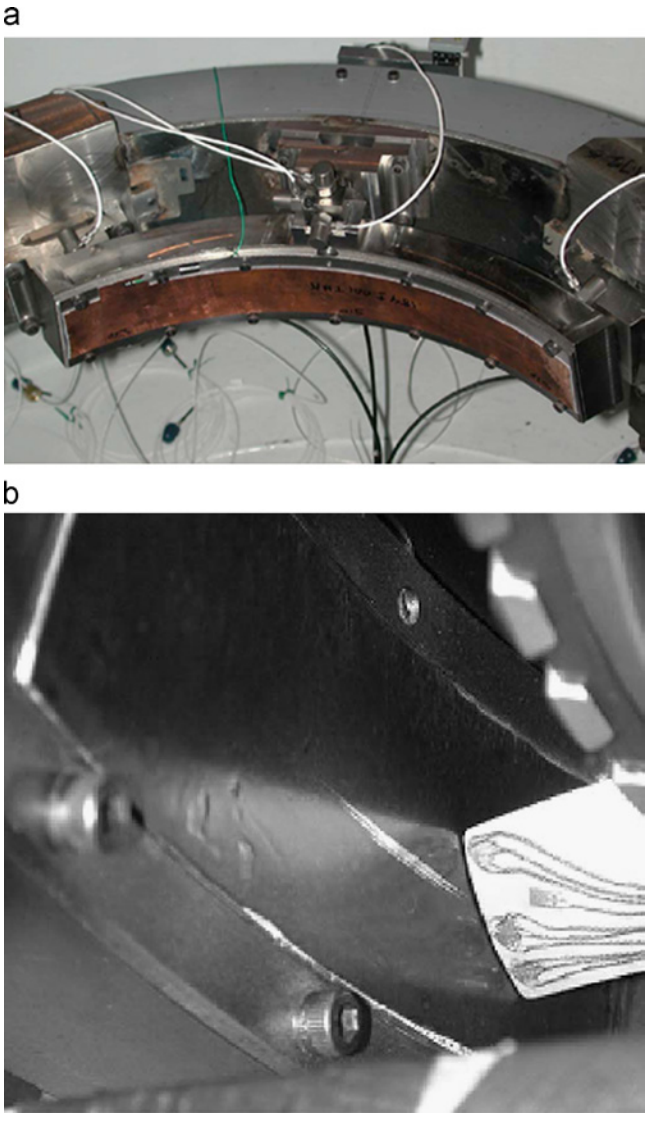

Fig. 9. Instrumentation of the OSU test bench [69]. (a) Casing with instruments and (b) blade equipped with temperature probe and deformation gages.

5.1. Blade-casing contact

Two types of test bench are used to study blade-casing contacts. The first are generally limited to a section of rigid and instrumented casing [68–72]. They use rotors with a single blade to facilitate the control of the contact process. These benches are equipped with pneumatic or electric actuators that allow varying the casing position and control the depth of

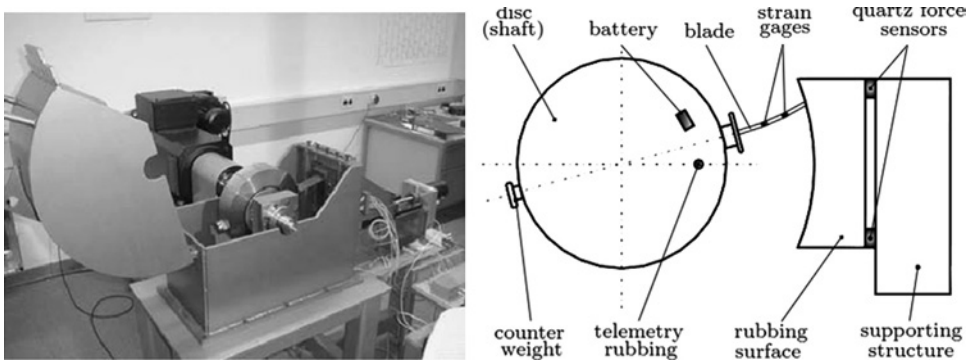

Fig. 10. Test bench of the University of Essen [72].

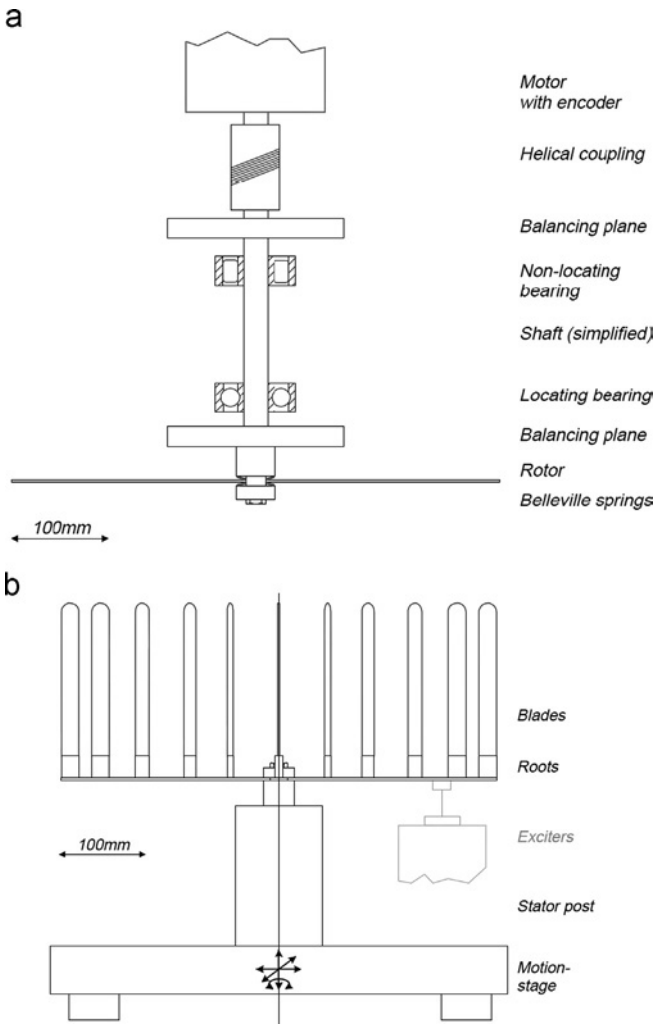

Fig. 11. Test setup [1]. Rotor (a) and stator (b).

contact penetration. The second type of test bench considers a complete bladed wheel and its casing [1,7,73]. Contact is induced either by vibratory excitation, or by reducing the clearance between the blade and the casing at standstill and then forcing the contact by centrifugal loading. The contact generally begins on an instrumented overlength blade.

The test bench developed by the Ohio State University (OSU) [68,70] is a very rigid bench with a single rotating blade driven by a pneumatic turbine up to a speed of 20,000 rpm (Fig. 8).

A segment of the casing is equipped with three triaxial piezoelectric force transducers. Measured transfer functions give the local forces transferred to contact points on the casing. Vibrations during contact are measured by five accelerometers, three for radial displacements and the two others for axial and angular displacements (Fig. 9(a)). The blade is equipped with deformation gages and thermocouples, at the tip and the root (Fig. 9(b)). The localization and extent of contacts are evaluated by analyzing the parts after testing and by using blue ink coating on the casing and the blade [70]. Two optical sensors detect blade passage and an electric circuit allows determining the number of contacts between the two parts [71].

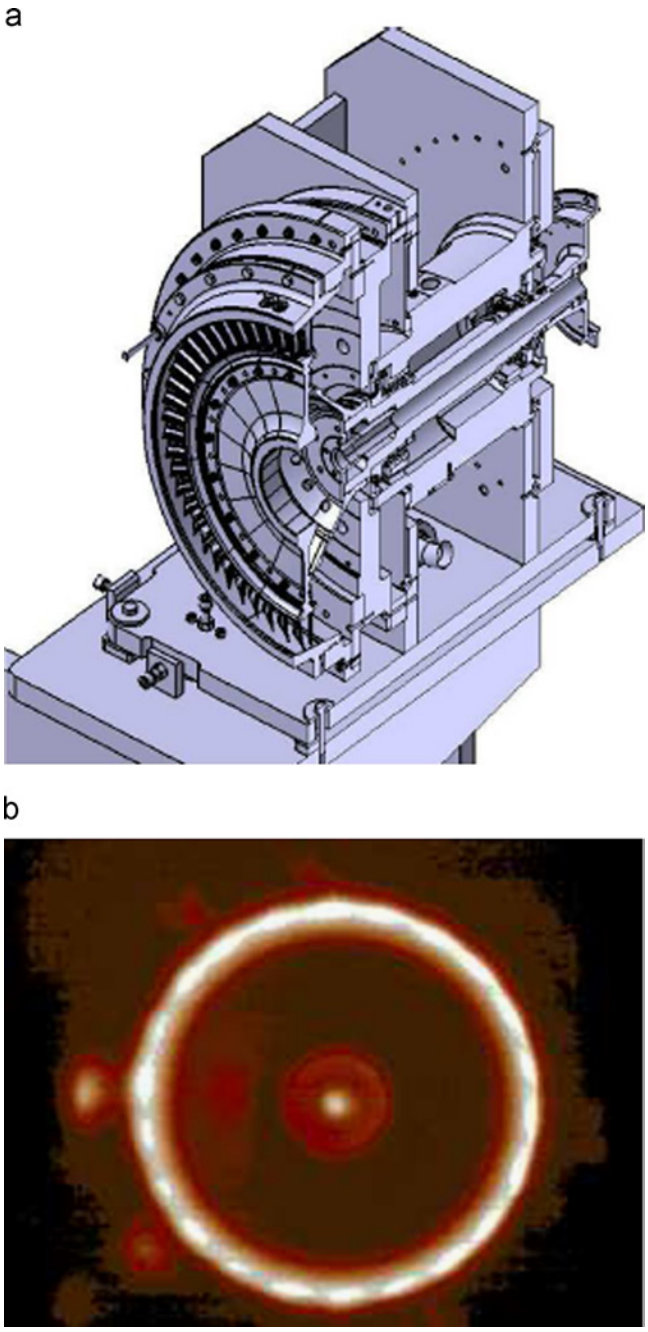

Fig. 12. Test bench of the NEWAC project, thermal field on the exterior of the casing [73].

Surprisingly, the different measurements show that the greatest stresses on the blade do not necessarily occur at the first passage. The measurements made by the deformation gages show that the blade is excited according to its first bending mode. The combination of axial, radial and circumferential blade deformations tends toward contact at the trailing edge. Padova [70,71] showed that the presence of abradable coatings on the casing considerably reduces contact forces and stresses in the blade.

The installation at the University of Essen [72] is dedicated to a rotor equipped with a blade instrumented with two deformation gages and telemetry transmission (Fig. 10). The contact force is measured by using biaxial piezoelectric sensors (axial and tangential directions) located at the contact surface and on the mounting. These measurements are similar to those performed by Padova.

Schmiechen [1] demonstrated experimentally the existence of a critical speed for which modal interaction occurs between rotor and stator, both flexible, leading to system instability. The experimental setup (Fig. 11) consists of a very simplified bladed wheel brought into contact with a flexible disc.

The wheel is fixed, facilitating instrumentation using eddy current displacement transducers and limiting aerodynamic effects. The contact is started by exciting the stator. The speed of the rotor is adjusted to satisfy the relation of interaction for a mode with two diameters. The rotor and the stator respond with high amplitudes that are maintained for a finite duration. The spectrum is dominated by the frequency given by the interaction diagram. Divergence is not visible on the time signals, as the amplitudes are limited due to structural nonlinearity. The existence of instability is therefore established. At sub- or supercritical speeds or in the presence of intentional unbalance, the amplitudes are significant but less regular and finally damped. Indeed, the transfer of the rotor's kinetic energy to the vibration energy of the rotor–stator system is lower than the energy dissipated by friction. The direction in which waves propagate, predicted by the analysis, was not considered, most likely because of the small number of transducers used. According to the authors, it has not been possible to observe other critical regimes with more nodal diameters (3ND,4ND,5ND) due to imperfections on the rotor. In addition, this study did not take into account wear or heat.

The NEWAC project (Fig. 12) is based on a test setup composed of a full HP compressor blisk mounted eccentrically on a spindle and driven electrically inside a casing with a coating [73]. The speed of the rotor is stabilized in relation to a modal interaction. Two minutes after the contact has been initialized a divergence of the deformation measured on the blade was observed. Wear on the abradable coating is characterized by lobes and measurement of thermal fields by infrared camera outside the casing also highlights a lobed temperature distribution. The number of these lobes is the same as the ratio of the frequencies involved, corresponding to the intermittent behavior described above.

Millecamps [7] focused on a stage of a low pressure axial compressor equipped with an overlong titanium blade held by a dovetail attachment and brought into contact with a titanium casing with an abradable coating. The contact was engaged, either dynamically by modal interaction, either by reducing blade-casing clearance at standstill and then by forcing the contact using the centrifugal effect. After a transient phase the response spectrum was dominated by the first flexion mode of the blade which diverged inducing an increase in temperature on the casing of 120 °C in 30 s. After the test, the analysis revealed a wear profile of the abradable coating with two circumferential lobes next to the leading edge linked to the ovalization of the casing and 6 or 7 lobes near the trailing edge. This number of lobes is equal to the ratio of the frequencies of the blade mode and the rotational speed. The analysis was completed in Refs. [15,16] by an axisymmetric finite element model of thermal conduction assuming a uniform circumferential distribution of heat flows at contact. The results obtained greatly depended on the hypothesis formulated on the axial localization of the heat flux. These tests confirm that the thermal expansion of the casing and wear play a major role in the occurrence of divergence.

5.2. Rotor–stator contact

For the rotor-casing contact, experimental conditions allowing the identification of the most critical operating modes and the zones of instability are not yet completely under control. However, the different results obtained on experimental test benches [20,21,26,34,59,74–76] confirm that dynamic behaviors can vary in intensity or evolve from one configuration to another as a function of different parameters, such as:

Friction between stator and rotor. Associated with unbalance, the friction coefficient induces the friction force between the rotor and the stator. Around the critical speed, forward whirl annular motion may evolve toward a backward whirl motion when the coefficient of friction is high. When the contact surface is lubricated the forward annular motion is maintained and no backward whirl motion occurs.

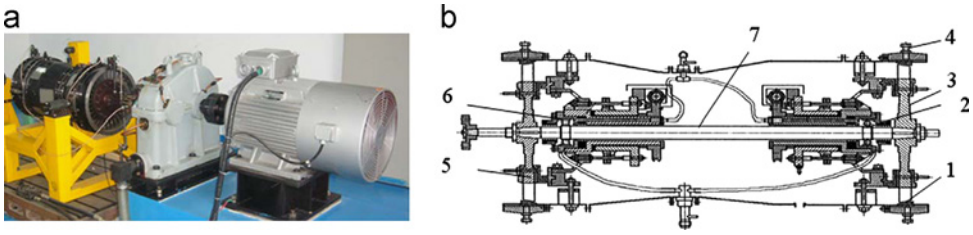

Fig. 13. Aircraft engine test bench [77].

Stator compliance and damping. The compliance of the stator, either natural or linked to more or less tight fixations has a large influence on the rotor's motion. When the stator is compliantly mounted, in case of dry friction whip, the rotor precesses at a frequency close to the combined frequency of the connected rotor and stator system. Signal analyses may show harmonic sidebands in addition to the main backward whirl/whip components that may be caused by support anisotropy [26]. Dai [76] showed that it is possible to design compliant motion limiting devices that allow to avoid full rubbing. Rotor–stator contact can also create a strong dynamic coupling phenomenon associated with the propagation of waves in the structure. This phenomenon occurs only with stators characterized by cyclic symmetry. Increasing damping brought by the stator reduces the occurrence of backward whirl.

Rotor/stator clearance. If the ratio between the clearance and the diameter of the shaft is low, rebounds are frequent and the behavior is rather unsteady. When clearance increases chaos tends to disappear. The more clearance there is, the greater the vibratory eccentricity necessary to exceed it is. Consequently the level of rotor excitation plays a major role and the shape of the rotor orbit becomes very sensitive to rotational speed.

Gyroscopic effect. It has been observed that the gyroscopic effect is generally negligible. Nonetheless, with a significant gyroscopic effect, it is possible to separate forward and backward modes. The gyroscopic effect is significant in the case of aircraft engines but less for low pressure stages of turbines where forward and backward modes remain very close.

Operating speed. For the same set of experimental parameters, the onset of vibratory behavior in forward or backward whirl appears to depend on prior speed conditions (rotor slowing down or speeding up). However, it is not possible to give a general conclusion.

Chen [77] used a test bench to reproduce the configuration of rotor–stator contact faults in aircraft engines. The prototype considered, presented in Fig. 13, is equivalent to a real turbine with a scale factor of one third. Experimental

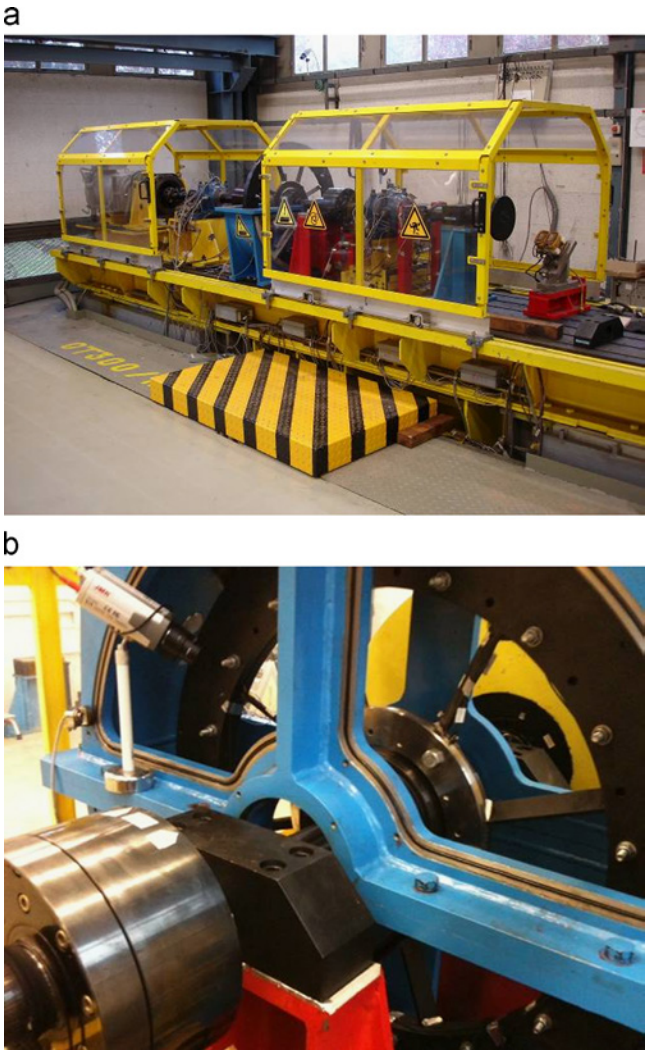

Fig. 14. EURoPE test bench (EDF R&D).

results confirm the presence of multi-harmonic frequency components when a rubbing fault occurs. As the possible rotating speed range is lower than the first critical speed fractional harmonic frequency components were not observed.

Choi [78] performed an experimental analysis on nonlinear superharmonic, subharmonic and jump phenomena using a test bench with intermittent contacts. The study compares the numerical results obtained from two contact models (linear penalization and restitution coefficient) with experimental results. The restitution parameters, the friction coefficient and the contact stiffness were adjusted experimentally. The numerical results closest to the test results in terms of vibration level and orbit shape are given by the penalized linear model. Experimental and numerical orbits differ sometimes during accelerations. This seems to indicate the existence of multiple responses that can give rise to jump, sub- and super-harmonics, and chaotic regimes.

Chu [79] used four different test benches, ranging from a simple single disc rotor to a multi-disc bi-rotor with a special stator structure, to obtain full annular rubbing. Rotor and stator concentricities are adjustable. Clearance is modified by interchanging the internal couplings to control the instant of contact and its severity. The results show nonlinear vibrations corresponding to light contact conditions (harmonics 1X and 2X with regular periodic motion), light and heavy contact with bifurcation (harmonics 1X, 2X, 1/2X and 3/2X with regular bi-periodic motion, and tri-periodic in certain configurations giving rise to harmonic 3X as well as fractional components 1/3X, 2/3X, 4/3X and 5/3X), heavy contact (irregular quasi-periodic motion with a continuous spectrum around harmonic 1X), and chaotic behavior. The stiffening effect of the contact is also observed.

Diangui [80] carried out rotor–stator contact experiments at different rotational speeds. The measurements of lateral vibrations conformed to the classical results in the literature. Regarding the behavior in torsion, the frequency measured during friction was greater than that without friction and reached a maximum threshold value.

Fumagalli [75] studied the contact between a rotor and several stators made of different materials (Graphite, Beryllium Bronze, Bronze, Nylon) associated with different suspension conditions. One interesting point considered was energy exchange between the two bodies. Part of the rotational energy is used to maintain the whirl, whereas the other part corresponded to thermal loss in the form of heat.

Bently [21] performed tests using steel/teflon contacts with forward whirl full annular rub and reverse precessional full annular rub (dry whip) between a rotor and a seal. The analysis focused on the jump phenomenon during forward whirl, the mechanism triggering rubbing during backward whirl, unbalance effects, the state of lubrication on the surface, rotational speed and seal rigidity. Considerable contact efforts are generated and local heating induced by friction severely deformed

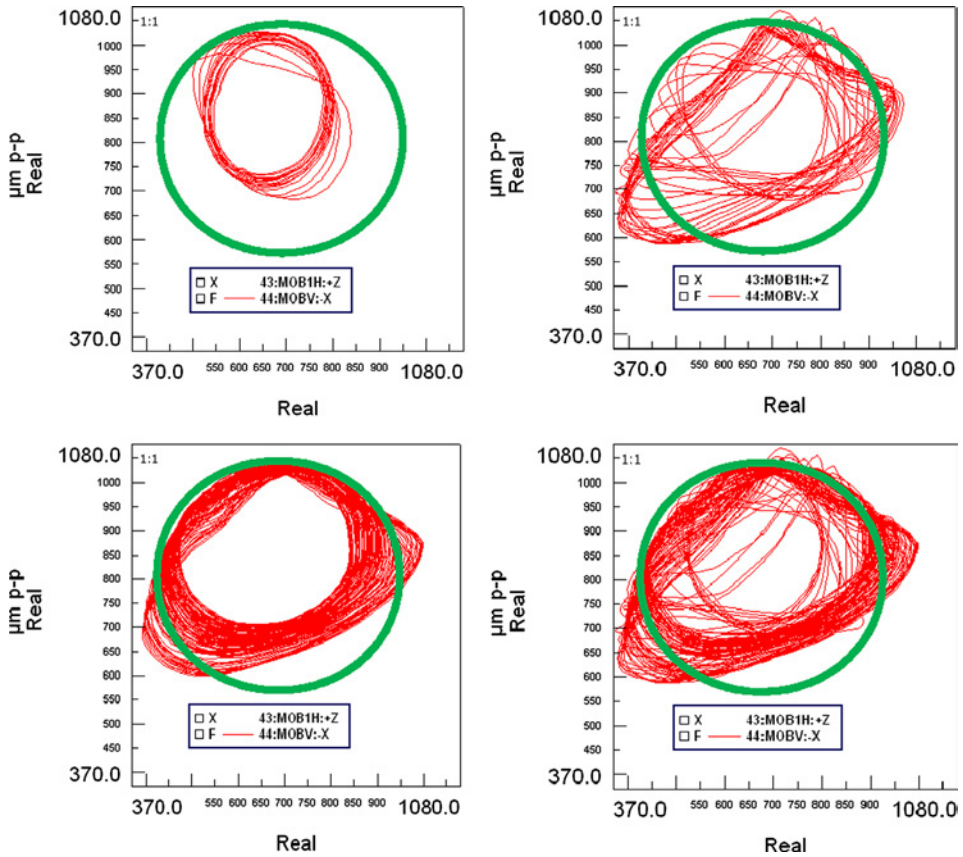

Fig. 15. Measured orbits compared to the clearance circle (test mass of 55.89 g).

the teflon seal and thus changed the normal direction of the contact as well as the equivalent friction coefficient. Forward whirl annular rub can transform into full annular rub with backward whirl around the resonance frequency when the rotor/seal friction coefficient reaches a high level in configurations with small rotor radius/clearance ratios (of the order of 10–40) even without external disturbance. In this case, the rotor comes into contact with the seal at an almost constant frequency; higher than the natural frequency of the rotor alone, but lower than the natural frequency of the coupled system. Once generated, rubbing in backward whirl continues throughout the range of rotational speeds if sliding persists.

The EURoPE test bench, developed at EDF R&D, is composed of a rotor rotating inside a fixed annular stator linked to a supporting structure [81] (Fig. 14). The rotor–stator contact here is generated by exciting the shaft via controlled unbalance forces. These forces are imposed on the shaft just before the deceleration phase while the machine is balanced during acceleration. The setup used to achieve this objective relies on a case, fixed to a flywheel, in which is placed a mass of ice (water). A compensatory mass is fixed at the opposite to balance the machine during acceleration. The machine is accelerated from rest, crosses the critical speed at 1350 rpm and is maintained at 1650 rpm until the ice melt and vibratory levels stabilize. Then the machine is sufficiently unbalanced to induce vibrational amplitudes exceeding the rotor–stator clearance (0.650 mm) and the engine power supply is switched off to allow the rotor to slow down freely.

The casing is fixed to the frame by 4 mounts. An interface part, made of different materials (brass, PTFE, steel), is used to adjust the rotor–stator gap. Force transducers are mounted between the interface and the casing to measure the forces generated by the contact. Four force transducers are used and the measurement is taken in the radial and tangential directions.

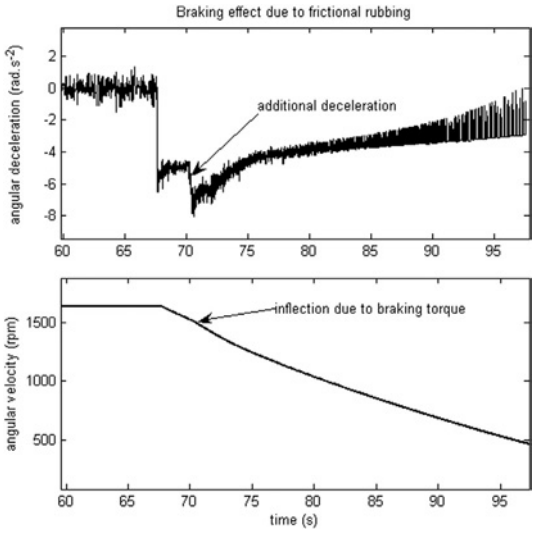

Fig. 16. Angular deceleration and velocity. Effect of braking due to contact.

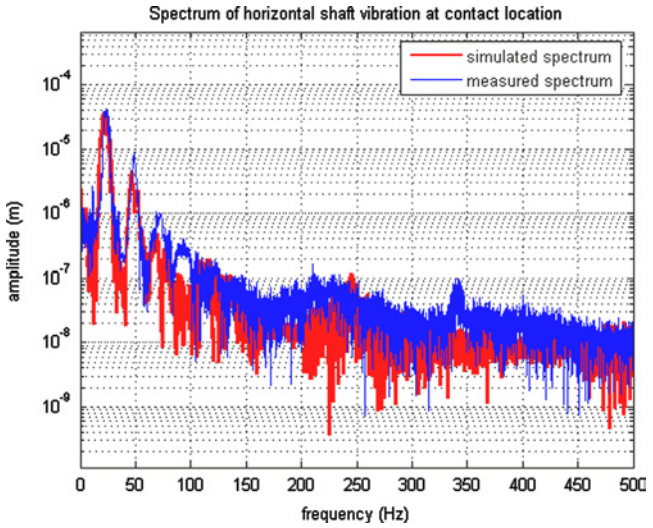

Fig. 17. Comparison of numerical and experimental frequency spectra.

The analysis of the signals measured during the test shows the occurrence of shocks on the force transducers on the stator when a speed of 1498 rpm is reached, then the beginning of stabilization at 1446 rpm and finally the disappearance of shocks below 1205 rpm. Then contact occurs between 1498 and 1205 rpm. Rotor–stator coupling causes an increase in critical speed of about 50 rpm. The images in Fig. 15 show the orbit of the rotor during the contact phase. The rotor orbits in clockwise direction. The contact starts in the upper part of the casing (image 1). The shape of the orbit changes quickly. Image 2 shows a triangular orbit lasting several revolutions and associated with three points of contact per revolution. The rotation of the orbit then continues, and there are only two contact points per revolution (image 3). Image 4 presents the whole process from 1531 to 1187 rpm.

The representation of the angular velocity and deceleration in Fig. 16 shows the first phase corresponding to the stabilized speed (up to 68 s) and the second phase of deceleration corresponding to the slowdown without contact when the engine power supply is switched off (from 68 to 70.5 s). Then, the third phase begins by a new brutal deceleration due to the initiation of contact at 1498 rpm and ends when contact disappears at 1205 rpm (from 70.5 to about 76 s). Finally the last phase, when contact is lost, shows a return to the natural deceleration associated to phase 2. As shown, there is a clear deceleration linked to braking caused by contact.

The numerical developments achieved by Roques [42] take into account the deceleration of the shaft line and considers all the significant parameters: contact force, stator flexibility, friction coefficient, torsion. Due to the significant eccentricity and out-of-roundness of the rotor (105 and 75 μm respectively at radius level), the map of the real clearances is integrated in the model. Slight touching and light contact configurations show that the numerical model reproduces the behavior observed on the bench very well (Fig. 17) [81].

For the shaft line considered, deceleration and transient contact are very rapid (less than 50 and 10 s respectively). These durations do not allow examining all the physical aspects involved by rotor–stator interactions on a real machine. The perspective is therefore to move toward a more severe and representative configuration including a flywheel, in order to ensure that the rotor–stator contact does not generate complex and yet non-controlled phenomena.

6. Conclusions

This study is aimed at evaluating the main works published on the problem of contact between fixed and moving parts of turbomachines, by focusing on the two principal configurations involving contact, namely blade-casing and rotor–stator. The analysis examined existing numerical models and experimental setups and highlighted the phenomenology involved during contacts. It confirmed the great complexity of the problems which by nature are considerably nonlinear due to the contacts and involve large displacements and deformations, substantial efforts in the bearing structures and induced plasticity. Moreover, the mechanisms are intrinsically multiphysical and multiscale, including local/global coupling of dynamic and thermomechanic responses, the effects of high speeds of rotation, and strong coupling between the global dynamics of the system and local phenomena that involve material and tribological characteristics (temperature, abradability, etc.).

The phenomenon of contact at blade tips is relatively well controlled and numerical models can now be used to correctly predict potential dynamic interactions between bladed wheels and casings. Due to the development of adapted reduction techniques, it is possible to obtain the response spectrum of bladed assemblies for a range of rotation speeds including contacts at acceptable cost. Current models should soon be enhanced by taking into account mistuning and gyroscopic effects.

The studies published focusing on rotor–stator contacts have led to major advances in understanding induced behaviors and their modeling. The different types of possible configurations are well known but only the most recent studies have really permitted identifying all the most influential parameters and the co-existence of several possible behaviors in certain operational areas. Unfortunately, most of the studies that have been published are based on very simplified models, for example, the Jeffcott type rotor and rigid bearings, and are not fully adapted to reproducing behaviors on real machines. Furthermore, in order to develop precise predictive analysis tools, it will be important to integrate the coupling of thermal, mechanical and wear parameters.

Acknowledgment

This work has been partially supported by the French National Research Agency (ANR) in the frame of its Technological Research COSINUS program. (IRINA, project ANR 09 COSI 008 01 IRINA).

References

[1] P. Schmiechen, Travelling Wave Speed Coincidence (Ph.D. thesis). Imperial College of London, 1997.
[2] S. Sinha, Dynamic characteristics of a flexible bladed-rotor with Coulomb damping due to tip-rub, J. Sound Vib. 273 (2004) 875–919.
[3] N. Lesaffre, J. Sinou, F. Thouverez, Model and stability analysis of a flexible bladed rotor, Int. J. Rotating Mach. (2006) 1–16.
[4] N. Lesaffre, Stabilité et Analyse Non-linéaire du Contact Rotor–Stator (Thèse de Doctorat). Ecole Centrale de Lyon, 2007.
[5] M. Legrand, Modèles de Prédiction de l'Interaction Rotor/Stator dans un Moteur d'Avion (Thèse de Doctorat). Ecole Centrale de Nantes, 2005.

[6] M. Legrand, C. Pierre, P. Cartraud, J.-P. Lombard, Two-dimensional modeling of an aircraft engine structural bladed disk–casing modal interaction, J. Sound Vib. 319 (2009) 366–391.
[7] A. Millecamps, J.F. Brunel, P. Dufrenoy, F. Garcin, M. Nucci, Etude Thermomécanique Du Contact Aube-Carter D'un Turboréacteur Et Conséquence Sur Son Excitation Dynamique. 19Ème congrès Français de Mécanique Marseille, 2009.
[8] M. Legrand, A. Batailly, C. Pierre, Numerical investigation of abradable coating removal in aircraft engines through plastic constitutive law, J. Comput. Nonlinear Dyn. 7 (2012). article 011010.
[9] R.J. Williams, Simulation of blade casing interaction phenomena in gas turbines resulting from heavy tip rubs using an implicit time marching method. in: Proceedings of ASME Turbo Expo, GT2011-45495, 2011.
[10] A. Batailly, Simulation De L'interaction Rotor/Stator Pour Des Turbomachines Aéronautiques En Configuration Non-Accidentelle (Thèse de Doctorat), Ecole Centrale de Nantes, 2008.
[11] A. Batailly, M. Legrand, P. Cartraud, C. Pierre, Assessment of reduced models for the detection of modal interaction through rotor stator contacts, J. Sound Vib. 329 (2010) 5546–5562.
[12] M. Legrand, A. Batailly, B. Magnain, P. Cartraud, C. Pierre, Full three dimensional investigation of structural contact interactions in turbomachines, J. Sound Vib. 331 (11) (2012) 2578–2601.
[13] N.X. Zheng And al., Development of air seal systems for modern jet engines, 2003; ⟨http://www.mtu.de/en/technologies/engineering_news/development/Zheng_Dglr2003_seal_system.pdf⟩.
[14] A. Batailly, M. Legrand, C. Pierre, Influence of abradable coating wear mechanical properties on rotor stator interaction. in: Proceedings of ASME Turbo Expo 2011, GT2011-45189, 2011.
[15] A. Millecamps, Interaction aube-carter: contribution de l'usure et de la thermomécanique sur la dynamique de l'aube (Thèse), Université Lille 1, 2010.
[16] A. Millecamps, J.F. Brunel, P. Dufrenoy, F. Garcin, M., Nucci, Influence of thermal effects during blade-casing contact experiments, in: Proceedings of the ASME International Design Engineering Technical Conference, vol. 1, 2010, pp. 855–862.
[17] A. Muszynska, Rotor-to-stationary element rub-related vibration phenomena in rotating machinery, Literature Suryey, The Shock and Vibration Digest 21-3 (1989) 3–11.
[18] A. MuszynskaRotordynamics, CRC Taylor & Francis Group, ISBN 0-8247-2399-6, Boca Raton, London, New York, Singapore, 2005, pp. 1–1120.
[19] S. Ahmad, Rotor casing contact phenomenon in rotor dynamics. Litterature survey, J. Vibration Control 16 (9) (2010) 1369–1377.
[20] A.R. Bartha, Dry Friction Backward Whirl of Rotors (Ph.D. Thesis), Swiss Federal Institute of Technology, Zurich, Dissertation ETH No. 13817, 2000.
[21] D.E. Bently, J.J Yu, P. Goldman, A. Muszynska, Full annular rub in mechanical seals, Part I: experimental results, Int. J. Rotating Mach. 8 (5) (2002) 319–328.
[22] M.O.T Cole, P.S. Keogh, Asynchronous periodic contact modes for rotor vibration within an annular clearance, J. Eng. Sci. ImechE 217 (Part C) (2003) 1101–1115.
[23] A Muszynska, P. Goldman, Chaotic responses of unbalanced rotor/bearing/stator systems with looseness or rubs, Chaos, Solitons and Fractals 5 (9) (1995) 1683–1704.
[24] A. Lingener, Experimental investigation of reverse whirl of a flexible rotor, in: Proceedings of the 3rd International conference on Rotordynamics IfToMM Lyon France, 1990, pp. 13–18.
[25] S.H. Crandall, From whirl to whip in rotordynamics, in: Proceedings of the 3rd International Conference on Rotordynamics IfToMM, Lyon France, 1990, pp. 19–24.
[26] J.C. Wilkes, D.W. Childs, B.J. Dyck, S.G. Phillips, The numerical and experimental characteristics of multimode dry-friction whip and whirl, J. Eng. Gas Turbines Power 132 (5) (2010). 052503-1-9.
[27] A. Bhattacharya, D.W. Childs, Dry-friction whirl and whip between a rotor and a stator: effect of rotor-stator coupling due to seals and rotor rigid-body dynamics, in: Proceedings of ASME Turbo Expo 2009 Orlando, GT2009-59979, 2009.
[28] D.W. Childs, A. Bhattacharya, Prediction of dry-friction whirl and whip between a rotor and a stator, J. Vib. Acoust. 129 (3) (2007) 355–362.
[29] M.O. Cole, On stability of rotor dynamic systems with rotor/stator contact interaction, in: Proceedings of the Royal Society A: Mathematical, Physical and Engineering Science, vol. 464–2100, 2008, pp. 3353–3375.
[30] G.X. Li, M.P. Païdoussi, Impact phenomena of rotor-casing dynamical systems, Nonlinear Dyn. 5 (1994) 53–70.
[31] J. Jiang, H. Ulbrich, Stability analysis of sliding whirl in a nonlinear Jeffcott rotor with cross-coupling stiffness coefficients, Nonlinear Dyn. 24 (2001) 269–283.
[32] J. Jiang, Determination of the global responses characteristics of a piecewise smooth dynamical system with contact, Nonlinear Dyn. 57 (2009) 351–361.
[33] Z. Shang, J. Jiang, L. Hong, The global responses characteristics of a rotor/stator rubbing system with dry friction effects, J. Sound Vib. 330 (2011) 2150–2160.
[34] Y.S. Choi, Investigation on the whirling motion of full annular rotor rub, J. Sound Vib. 258 (1) (2002) 191–198.
[35] P. Pennacchi, N. Bachschmid, E. Tanzi, Light and short arc rubs in rotating machines: experimental tests and modelling, Mech. Syst. Signal Process. 23 (2009) 2205–2227.
[36] Y.S. Choi, Dynamics of rotor rub in annular clearance with experimental evaluation, J. Mech. Sci. Technol. 8 (4) (1994) 404–413.
[37] S. Popprath, H. Ecker, Nonlinear dynamics of a rotor contacting an elastically suspended stator, J. Sound Vib. 308 (3–5) (2007) 767–784.
[38] F. Choy, J. Padovan, Non-linear transient analysis of rotorcasing rub events, J. Sound Vib. 113 (3) (1987) 529–545.
[39] B.O. Al-Bedoor, Transient torsional and lateral vibrations of unbalanced rotors with rotor-to-stator rubbing, J. Sound Vib. 229 (3) (2000) 627–645.
[40] T.H. Patel, A.K. Darpe, Coupled bending-torsional vibration analysis of rotor withrub and crack, J. Sound Vib. 326 (3–5) (2009) 740–752.
[41] O. Grapis, V. Tamuzs, N.-G. Ohlson, J. Andersons, Overcritical high-speed rotor systems, full annular rub and accident, J. Sound Vib. 290 (3–5) (2006) 910–927.
[42] S. Roques, Modélisation du Comportement Dynamique Couplé Rotor-Stator d'une Turbine en Situation Accidentelle (Thèse de Doctorat). Ecole Centrale de Nantes, 2007.
[43] S. Roques, M. Legrand, P. Cartraud, C. Stoisser, C. Pierre, Modeling of a rotor speed transient response with radial rubbing, J. Sound Vib. 329 (5) (2010) 527–546.
[44] S. Braut, R. Zigulic, A. Skoblar, G. Stimac, M. Butkovic, M. Jokic, Dynamic Analysis of the Rotor–Stator Contact due to Blade Loss, in: Proceedings of the 12th IFToMM World Congress, Besançon France, 2007.
[45] N. Bachschmid, P. Pennacchi, A. Vania, Thermally induced vibrations due to rub in real rotors, J. Sound Vib. 299 (2007) 683–719.
[46] J. Sawicki, A. Montilla-Bravo, Thermomechanical behavior of rotor with rubbing, Int. J. Rotating Mach. 9 (1) (2003) 41–47.
[47] B.L. Newkirk, Shaft rubbing: relative freedom of rotor shafts from sensitiveness to rubbing contact when running above their critical speeds, Mech. Eng. 48 (8) (1926) 830–832.
[48] D. Childs, A note on Kellenberger's model for spiral vibrations, J. Vib. Acoust. 123 (2001) 405–408.
[49] H.A. Abdel-Aal, Efficiency of thermal energy dissipation in dry rubbing, Wear 255 (2003) 348–364.
[50] J. Denape, N. Laraqi, Aspect thermique du frottement: mise en évidence expérimentale et éléments de modélisation, Méc. Ind. 1 (2000) 563–579.
[51] I. Temizer, P. Wriggers, Thermal contact conductance characterization via computational contact homogenization: a finite deformation theory framework, Int. J. Numer. Methods Eng. 83 (1) (2010) 27–58.
[52] E. Kosing, R. Scharl, H. Schmuhl, Design improvements of the EJ200 HP compressor. From design verification engine to a future all blisk version, in: Proceedings of ASME TURBO EXPO, GT2001-0283, 2001.
[53] D. Japikse, Decisive factors in advanced centrifugal compressor design and development, ASME PID 5 (2000) 23–36.
[54] G.F. Zhang, W.N. Xu, W. Zhang, Analytical study of nonlinear synchronous full annular rub motion of flexible rotorstator system and its dynamic stability, Nonlinear Dyn. 57 (2009) 579–592.
[55] F. Cong, J. Chen, G. Dong, K. Huang, Experimental validation of impact energy model for the rub–impact assessment in a rotor system, Mech. Syst. Signal Process. 25 (2011) 2549–2558.
[56] P. Wriggers, Nonlinear Finite Element Methods, Springer Berlin Heidelberg, 560.
[57] R.M. Brach, Mechanical Impact Dynamics: Rigid Body Collisions, Wiley, New York260.

[58] E. Rivin, Stiffness and Damping in Mechanical Design, Marcel Dekker, New York, 512.
[59] F. Chu, W. Lu, Stiffening effect of the rotor during the rotor-to-stator rub in a rotating machine, J. Sound Vib. 308 (3–5) (2007) 758–766.
[60] G. Von Groll, D. Ewins, The harmonic balance method with arc-length continuation in rotor/ stator contact problems, J. Sound Vib. 241 (2) (2001) 223–233.
[61] F. Chu, Z. Zhang, Bifurcation and chaos in a rub impact Jeffcott rotor system, J. Sound Vib. 210 (1) (1998) 1–18.
[62] Y.B. Kim, S.T. Noah, Quasi periodic response and stability analysis for a non linera Jeffcott rotor, J. Sound Vib. 190 (2) (1996) 239–253.
[63] S. Edwards, A.W. Lees, M.I. Friswell, The influence of torsion on rotor/stator contact in rotating machinery, J. Sound Vib. 225 (4) (1999) 767–778.
[64] Z. Feng, X.Z. Zhang, Rubbing phenomena in rotor–stator contact, Chaos, Solitons Fractals 14 (2) (2002) 257–267.
[65] F. Chu, Z. Zhang, Periodic, quasi-periodic and chaotic vibrations of a rub-impact rotor system supported on oil film bearings, Int. J. Eng. Sci. 35 (10–11) (1997) 963–973.
[66] W. Qin, G. Chen, G. Meng, Nonlinear responses of a rub impact overhung rotor, Chaos, Solitons Fractals 19 (5) (2004) 1161–1172.
[67] S.L. Chen, M. Géradin, Finite element simulation of non-linear transient response due to rotor–stator contact, Eng. Comput. 14 (6) (1997) 591–603.
[68] C. Padova, J. Barton, M.G. Dunn, S. Manwaring, G. Young, M. Adams Jr., M. Adams, Development of an experimental capability to produce controlled blade tip/shroud rubs at engine speed, J. Turbomach. 127 (2005) 727–735.
[69] C. Padova, J. Barton, M.G. Dunn, S. Manwaring, Experimental results from controlled blade tip/shroud rubs at engine speed, J. Turbomach. 129 (2007) 713–723.
[70] C. Padova, M.G. Dunn, J. Barton, K. Turner, A. Turner, D. DiTommaso, Casing treatment and blade-tip configuration effects on controlled gas turbine blade tip/shroud rubs at engine conditions, J. Turbomach. 133 (2011) 713–723. article 011016.
[71] C. Padova, M. Dunn, J. Barton, T. Steen, K. Turner, Controlled fan blade tip/shroud rubs at engine conditions. ASME Turbo Expo Vancouver Canada, paper GT2011-45223, 2011.
[72] I. Krajcin, D. Söffker, Model-Based Estimation of Contact Forces in Rotating Machines. in: Proceedings of the 4th IMACS Symposium on Mathematical Modeling, Vienna University of Technology, Austria, February 5–7, 2003, 6 p.
[73] H. Reiss, Flow Control Core, Overview European Workshop on New Aero Engine Concepts, Munich, 30 June–1 July 2010.
[74] O. Ismeurt, Contribution à l'étude de l'influence du frottement rotor/stator sur le comportement dynamique des machines tournantes (Thèse de doctorat), INSA, Lyon France, 1995.
[75] M.A. Fumagalli, Modelling and measurement analysis of the contact Interaction between a high speed rotor and its stator. Thesis, Swiss Institute of Technology, 1997.
[76] X. Dai, Z. Jin, X. Zhang, Dynamic behavior of the full rotorstop rubbing: numerical simulation and experimental verification, J. Sound Vib. 251 (5) (2002) 807–822.
[77] G. Chen, C.G. Li, D.Y. Wang, Nonlinear dynamic analysis and experiment verification of rotor-ball bearings-support-stator coupling system for aeroengine with rubbing coupling faults, J. Eng. Gas Turbines Power 132 (2) (2010). article 022501 (9 pages).
[78] Y.-S. Choi, C.-Y. Bae, Nonlinear dynamic analysis of partial rotor rub with experimental observations, in: Proceedings of ASME Design Engineering Technical Conference, Pittsburgh, 2001.
[79] F. Chu, W. Lu, Experimental observation of nonlinear vibrations in a rub-impact rotor system, J. Sound Vib. 283 (3–5) (2005) 621–643.
[80] H. Diangui, Experiment on the characteristics of torsional vibration of rotor-to-stator rub in turbomachinery, Tribol. Int. 33 (2) (2000) 75–79.
[81] M. Torkhani, L. May, P. Voinis, Light, medium and heavy partial rubs during speed transients of rotating machines: numerical simulation and experimental observation, Mech. Syst. Signal Process. 29 (2012) 45–66.